JOURNAL OF SOLID STATE CHEMISTRY 87, 350–359 (1990)

The Luminescence of Europium(III) and Cerium(III) in Calcium Sulfate: Activators with an Effective Charge

D. VAN DER VOORT AND G. BLASSE

Debye Research Institute, University of Utrecht, P.O. Box 80000, 3508 TA Utrecht, The Netherlands

Received November 27, 1989

The luminescence and the quantum efficiency of the phosphors $CaSO_4:Eu^{3+}$ and $CaSO_4:Ce^{3+}$ are reported. The Eu^{3+} phosphor shows a very weak luminescence under charge-transfer excitation, the quantum efficiency amounting to about 10%. Codoping of the Eu^{3+} phosphor with P^{5+} or Na^+ as charge compensators enhances the luminescence efficiency. This is ascribed to a decrease of the concentration of vacancies in the lattice. The phosphor $CaSO_4:Ce^{3+}$ shows a very efficient ultraviolet luminescence. The Stokes shift of the *d–f* emission amounts to about 800 cm^{-1}. Vibrational structure is observed in the emission and excitation spectra. It is shown that the effective charge on the activator ion has a different influence on the relaxation of the opposite-parity excited states of Eu^{3+} and Ce^{3+}.

1. Introduction

During the last decades many Eu^{3+}-activated phosphors have been studied in which the Eu^{3+} ion replaces the chemically equivalent rare earth (RE) ions Gd^{3+} (*1*, *2*), La^{3+} (*3–5*), or Y^{3+} (*6–8*) of the host lattice. These ions offer a good fit for the Eu^{3+} ion, since the ions are of comparable size and the valencies are the same. Many of these phosphors have high quantum efficiencies. For example, the phosphor $Y_2O_3:Eu^{3+}$ (*8*) is used in several kinds of luminescent lamps. As far as we are aware there are no studies available which deal fundamentally with the possible influence of an effective charge on the luminescence of the Eu^{3+}activator. Such a situation occurs if Eu^{3+} is introduced in, e.g., a calcium compound. Although the sizes of Eu^{3+} and Ca^{2+} are not much different, their valencies are. The Eu^{3+} ion carries an effective positive charge in such a compound (*9*). This positive charge requires charge compensation. In this paper we report on the luminescence of Eu^{3+} and Ce^{3+} in $CaSO_4$.

$CaSO_4:Eu^{3+}$ has already been studied as a thermoluminescent material (*10–12*) which offers the possibility for dosimetric application. In crystals of $CaSO_4$ valence conversion of Eu(III) into Eu(II) has been observed (*13*, *14*). The RE ions in this lattice have been investigated using optical and EPR techniques (*15*). One of us studied the luminescence characteristics of Eu^{3+}–VO_4^{3-} pairs in $CaSO_4$ (*16*). Excitation into the vanadate group yields very efficient Eu^{3+} luminescence.

In this study the luminescence of the Eu^{3+}

0022-4596/90 $3.00

ion in $CaSO_4$ is investigated. An estimate of the quantum efficiency under charge-transfer (CT) excitation is made because the presence of an effective charge may be expected to influence the CT state. Of further interest is the influence of charge compensators on the luminescence characteristics of the Eu^{3+} ion in the $CaSO_4$ lattice.

In order to study the behavior of a luminescent *d–f* transition of a trivalent RE ion on a sublattice of divalent ions, the phosphor $CaSO_4:Ce^{3+}$ is also investigated.

The anhydrite crystal structure of $CaSO_4$ is well known (*17*). The unit cell is orthorhombic with a slight departure from tetragonal symmetry. The Ca^{2+} ions occupy a single crystallographic site with an eightfold oxygen coordination and site symmetry C_{2v}. The shortest cation–cation distance in this lattice is 3.5 Å.

It turns out that the quantum efficiency of the Eu^{3+} luminescence in $CaSO_4$ is low, viz. 10%. The efficiency can be enhanced by suitable charge compensators.The luminescence of the Ce^{3+} ion in $CaSO_4$, however, is very efficient.

2. Experimental

2.1 Preparation

All measurements described in this paper are performed on powdered samples. The Eu^{3+} phosphors were prepared by solid state reactions. In the system $Ca_{1-1.5x}Eu_xSO_4$ the samples with $x = 0.001$ and 0.005 were prepared; in the system $Ca_{1-x}Eu_xS_{1-x}P_xO_4$, samples with $x = 0.001$ and 0.003; and in the system $Ca_{2(1-x)}Eu_xNa_x(SO_4)_2$, samples with $x = 0.001$, 0.005, and 0.01. The starting materials were Eu_2O_3 (Highways Int., 99.999%), $CaCO_3$ (Merck, Suprapur), $(NH_4)_2HPO_4$, $(NH_4)_2SO_4$, and Na_2CO_3 (all from Merck, PA).

Stoichiometric amounts of the starting materials with 20 mol% excess of $(NH_4)_2SO_4$ were mixed in a ball mill and fired at 1000°C for 2 hr in air. The white powder was ground and fired again at 1000°C for 2 hr. The maximum doping concentration of Eu^{3+} in $CaSO_4$ without the addition of charge compensators lies between 0.5 and 1.0%.

Since it was not possible to prepare the phosphor $CaSO_4:Ce^{3+}$ by a solid state reaction as described above, an alternate method was used. Hereto $Ce_2(CO_3)_3 \cdot 5H_2O$ (Highways Int., 99.99%) was dissolved in a diluted hydrochloric acid solution (Baker Reagents). An appropriate amount of $CaCl_2$ (Merck) solution was added in order to obtain a 0.1% solution of Ce^{3+} toward Ca^{2+}. Under stirring and heating a concentrated sulfuric acid solution was added. A white precipitate was formed and washed thoroughly with distilled water and dried for several hours in air at 140°C.

The structure of the powders was checked with X-ray powder diffraction using Cu$K\alpha$ radiation.

2.2 Instrumentation

Diffuse reflection spectra of the powdered samples were recorded with a Perkin–Elmer Lambda 7 UV/VIS spectrophotometer. The instrumentation for recording excitation and emission spectra from 250 to 800 nm and the instrumentation for high resolution spectroscopy are described in Ref. (*18*).

The instrumental setup for the measurement of excitation spectra from 190 nm towards longer wavelengths consists of a water-cooled Hamamatsu 200 W Deuterium lamp as a light source and a Carl Leiss grating monochromator for excitation wavelength selection. A filter set was used for selection of the emission wavelength. The emission signal was detected with an RCA 31034 photomultiplier.

The excitation spectra were corrected for the output of the light sources. The emission spectra were corrected for the sensitivity of the photomultipliers.

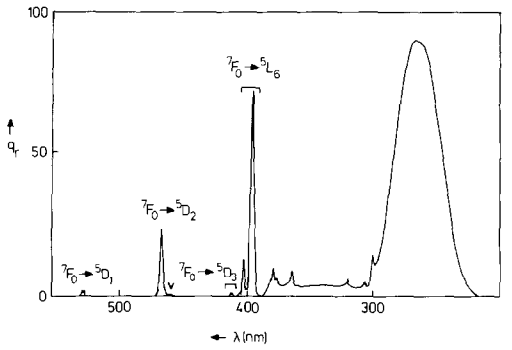

FIG. 1. Excitation spectrum of the Eu^{3+} emission in $CaSO_4:Eu^{3+}$ (0.5%) at 4.2 K. λ_{em} = nm. v indicates a vibronic transition. q_r gives the relative quantum output in arbitrary units.

3. Results

3.1 $CaSO_4:Eu^{3+}$ (Na^+ or P^{5+})

The diffuse reflection spectra of the phosphors, recorded at room temperature, show a broad band absorption in the ultraviolet region with a maximum at 260 nm. In the UV and visible region some very weak line absorptions are observed as well.

The excitation spectrum of the Eu^{3+} emission in $CaSO_4$ at 4.2 K is shown in Fig. 1 and is substantially the same as the reflection spectrum. The sharp lines belong to transitions within the $4f^6$ configuration of the Eu^{3+} ion starting from the $^7F_0$ ground state. In the $^7F_0 \rightarrow {}^5D_2$ region a vibronic transition is observed, positioned at 400 cm^{-1} from the electronic origin. Closer examination of the excitation spectrum in this region also reveals vibronic transitions at 1100 cm^{-1} from the electronic origin. The broad band at 260 nm is ascribed to an O^{2-}–Eu^{3+} CT transition and coincides with the absorption band in the reflection spectrum. The broad continuum from 300 to 380 nm originates from the presence of Eu^{2+} in the crystal lattice. Excitation in this region results in a broad band emission at 385 nm, ascribed to the $4f^65d \rightarrow 4f^7$ transition of the Eu^{2+} ion (*19, 20*), and a slight amount of Eu^{3+} emission. From the diffuse reflection spectrum it follows that about 1% of the Eu ions is incorporated into the $CaSO_4$ lattice in the divalent state.

In contrast to measurements by Danby (*13*) and Nambi and Bapat (*14*) we did not observe any conversion of Eu^{3+} into Eu^{2+} under continuous UV irradiation.

The Eu^{3+} emission in $CaSO_4$ under excitation into the CT band at 4.2 K is shown in Fig. 2. Only emission from the $^5D_0$ level is observed. In the $^5D_0 \rightarrow {}^7F_2$ region some vibronic transitions up to 1100 cm^{-1} from the electronic origin are observed. In the shorter wavelength region a weak Eu^{2+} emission is observed.

Excitation into the CT band at different wavelengths results in slightly different emissions in the $^5D_0 \rightarrow {}^7F_2$ region (as shown in Figs. 3a, 3b, 3c, and 3d). In order to excite all Eu^{3+} ions in the sample, an aselect excitation in the $^7F_0 \rightarrow {}^5L_6$ level was carried out. In Figs. 3e and 3f the emissions in the $^5D_0 \rightarrow {}^7F_{0,1}$ region under CT and $^7F_0 \rightarrow {}^5L_6$ excitation are shown, revealing a considerable

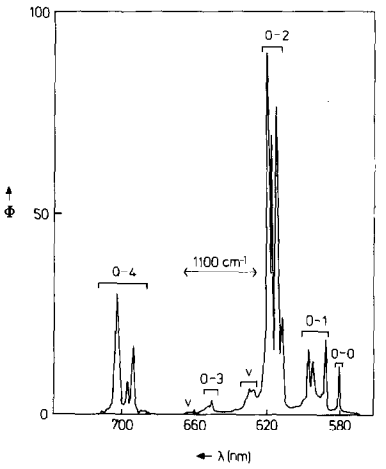

FIG. 2. Emission spectrum of $CaSO_4:Eu^{3+}$ under CT excitation (260 nm) at 4.2 K. Φ gives the spectral radiant power per constant wavelength interval in arbitrary units. In the figure the $^5D_0 \rightarrow {}^7F_J$ transitions are indicated. v indicates vibronic transitions.

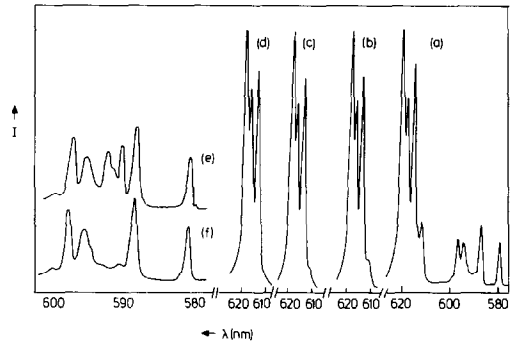

FIG. 3. Eu^{3+} emission in $CaSO_4$ for different excitation wavelengths. a–d show the changing $^5D_0 \rightarrow {}^7F_2$ emission under excitation at different wavelengths in the CT region: (a) 265 nm, (b) 270 nm, (c) 275 nm, (d) 280 nm. e and f show the difference in the $^5D_0 \rightarrow {}^7F_{0,1}$ emission between excitation at 395 nm ($^7F_0 \rightarrow {}^5L_6$) and 260 nm (CT band), respectively.

difference in the $^5D_0 \rightarrow {}^7F_1$ transition. The luminescence characteristics of $CaSO_4$ doped with 0.1% Eu^{3+} are the same as with 0.5% Eu^{3+}.

The excitation spectrum of $CaSO_4:Eu^{3+},P^{5+}$ (0.3%) is comparable to that of $CaSO_4:Eu^{3+}$ with a CT band at 260 nm and some sharp lines in the visible and UV. Excitation in the CT region, however, results in a very different emission spectrum. The emission spectrum is independent of the wavelength selection in the CT region and is the same under $^7F_0 \rightarrow {}^5L_6$ excitation. This behavior is also found for $CaSO_4:Eu^{3+}$, Na^+ (0.5%). While the excitation spectrum does not reveal any change, the emission spectrum of $CaSO_4:Eu^{3+}$, Na^+ under CT excitation is different from those of $CaSO_4:Eu^{3+}$ and of $CaSO_4:Eu^{3+}$, P^{5+}. Figure 4 pictures the emission spectra of the Eu phosphor without and the two Eu phosphors with charge compensation in the $^5D_0 \rightarrow {}^7F_{0,1,2}$ region under excitation into the CT band at 260 nm.

The excitation spectra of the three phosphors in the short wavelength region are depicted in Fig. 5. These spectra offer the possibility of a more accurate estimate of the position of the CT band than is possible from the excitation spectra recorded with the xenon lamp. This is due to the fact that the xenon lamp shows, in contrast to the deuterium lamp, a rapid intensity decrease in the CT region. The shorter wavelength spectra do not only reveal the position of the Eu^{3+} CT band, but show also a second broad excitation band at about 220 nm. This excitation band coincides with the observed absorption in the diffuse reflection spectrum of pure $CaSO_4$ and is therefore ascribed to excitation in the host lattice followed by energy transfer to the Eu^{3+} ion.

3.2 $CaSO_4:Ce^{3+}$

The Ce^{3+} ion in $CaSO_4$ shows a strong ultraviolet luminescence at 4.2 as well at 300 K. The excitation spectrum of the Ce^{3+} emission at 4.2 K is shown in Fig. 6. Four broad bands are observed with maxima at 297, 290, 269, 253, and 240 nm. The bands are ascribed to transitions from the $^2F_{5/2}$ ground state of the Ce^{3+} ion ($4f^1$) to the crystal-field split $5d$ level. The excitation

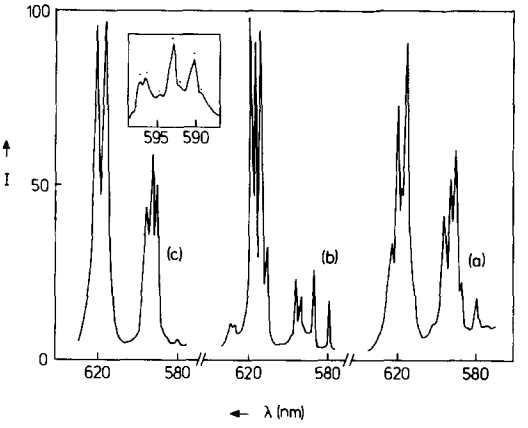

FIG. 4. Eu^{3+} emission in the $^5D_0 \rightarrow {}^7F_{0,1,2}$ region for (a) $CaSO_4:Eu^{3+}$, P^{5+}; (b) $CaSO_4:Eu^{3+}$; and (c) $CaSO_4:Eu^{3+}$, Na^+. Excitation takes place in the CT band at 260 nm. The inset shows the emission for $CaSO_4:Eu^{3+},Na^+$ with higher resolution.

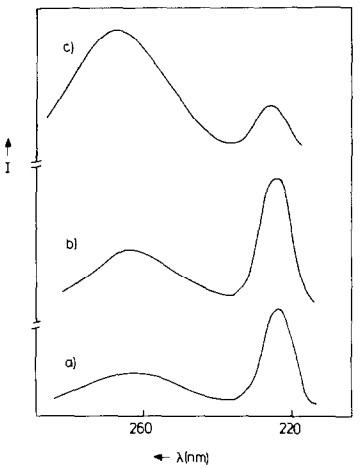

FIG. 5. Excitation spectra of the Eu^{3+} emission in the short wavelength region for (a) $CaSO_4:Eu^{3+}$; (b) $CaSO_4:Eu^{3+}$, P^{5+}; and (c) $CaSO_4:Eu^{3+}$, Na^+.

band on the longer wavelength side reveals a vibronic structure (see also Fig. 7). The zero-phonon line at 300.7 nm has some phonon replicas which are separated by intervals of 218 (±5) cm^{-1}.

The emission of Ce^{3+} in $CaSO_4$ at 4.2 K is also depicted in Fig. 7. It consists of two broad bands with maxima at 304 nm (32,900 cm^{-1}) and 325 nm (30,800 cm^{-1}), belonging to transitions from the lowest lying 5*d* level to the $^2F_{5/2}$ and the $^2F_{7/2}$ level of the 4*f* state. The Stokes shift amounts to about 800 cm^{-1}. The emission with a maximum at 304 nm shows two clearly observable zero-phonon transitions followed by vibronic structure. The phonon replicas are separated by intervals of 237 (±5) cm^{-1}. The two zero-phonon transitions have a separation which has almost the same value. This causes an overlap of the two progressions. The broad emission band with a maximum at 325nm has two clearly observable zero phonon transitions, but no distinct progression mode can be derived from the spectrum.

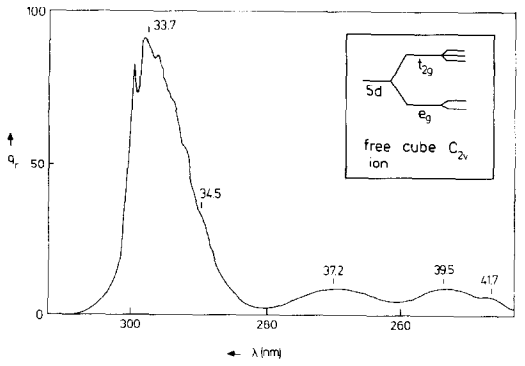

FIG. 6. Excitation spectrum of the Ce^{3+} emission in $CaSO_4$ at 4.2 K. λ_{em} = 324 nm. In the picture the wavenumbers of the excitation maxima are given in $cm^{-1}/1000$. The inset shows the splitting of the 5*d* level in cubic and C_{2v} site symmetry.

4. Discussion

4.1 $CaSO_4:Eu^{3+}$ (Na^+ or P^{5+})

4.1.1 Luminescence spectra. The excitation spectra of the Eu^{3+} luminescence in the $CaSO_4$ phosphors show the presence of Eu^{2+} in the samples (which transfer part of its excitation energy to Eu^{3+}). The $Eu^{2+} \rightarrow Eu^{3+}$ transfer is favored by a large spectral overlap between the Eu^{2+} emission and the relatively strong $^7F_0 \rightarrow {}^5L_6$ transition of the Eu^{3+} ion. In our solid state reaction technique we were not able to avoid the presence of Eu^{2+}, not even by heating in a pure oxygen atmosphere. The presence of Eu^{2+} most probably originates from the fact that the divalent sublattice is a suitable host for divalent cations.

Although the incorporation of charge compensators does not show any detectable influence on the amount of Eu^{2+} in the samples, the presence of Na^+ does affect the solubility of Eu^{3+} in $CaSO_4$. Preparation of $CaSO_4:Eu^{3+}$ (1%) yields a small amount of a second phase which can be ascribed to Eu_2O_3. In $CaSO_4:Eu^{3+}$, Na^+ (1%) this second phase was not observed.

The Eu^{3+} emission in $CaSO_4$ is observed only from the $^5D_0$ level. This means that multiphonon relaxation of the type $^5D_J \rightarrow$

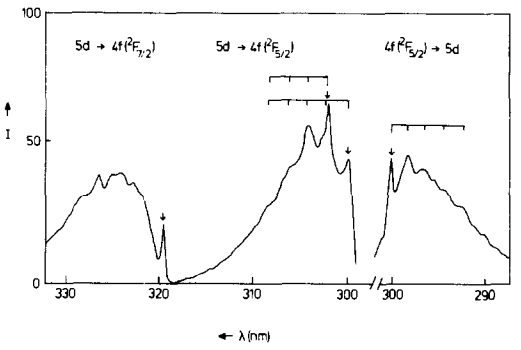

FIG. 7. Emission spectrum of $CaSO_4:Ce^{3+}$ at 4.2 K (left-hand side, $\lambda_{exc} = 290$ nm) and the longer wavelength excitation band of this emission (right-hand side, $\lambda_{em} = 324$ nm). The arrows indicate zero-phonon transitions. Vibrational progressions are also shown.

$^5D_{J-1}$ is an effective process in this lattice. This is ascribed to the presence of vibration frequencies up to 1100 cm^{-1} in this lattice. These frequencies are observed in some vibronic transitions in the neighborhood of the electronic $^7F_0 \rightarrow {}^5D_2$ and $^5D_0 \rightarrow {}^7F_2$ transitions. The vibrational mode with a frequency of about 400 cm^{-1} is ascribed to a coupling of the electronic transition with the vibration of the Eu^{3+} ion relative to the sulfate groups. The vibrational frequency of 1100 cm^{-1} belongs to the asymmetrical breathing vibration of the sulfate group (ν_3). The intensity of the vibronic transitions is weak. In the excitation and emission spectra the vibronic transitions are of comparable strength.

If the Eu^{3+} ion in $CaSO_4$ has the same site symmetry as Ca^{2+} (C_{2v}), splittings in one, three, and four lines are expected for the $^5D_o \rightarrow {}^7F_{0,1,2}$ transitions, respectively. The dominating emission of Eu^{3+}, shown in Fig. 2, consists of one, three, and three lines for the $^5D_0 \rightarrow {}^7F_{0,1,2}$ transition. In Fig. 3 four lines are visible in the $^5D_0 \rightarrow {}^7F_2$ transition, but from Fig. 3 it follows that the weakest peak belongs to another Eu^{3+} site. From the dominating emission under CT excitation we conclude that this emission is due to an Eu^{3+} ion in C_{2v} site symmetry. The assumption for this assignment is the fact that one of the four lines in the $^5D_0 \rightarrow {}^7F_2$ transition is obscured, due to an insufficient resolution. The observed emission of Eu^{3+} in $CaSO_4$ is mainly due to electric dipole transitions ($^5D_0 \rightarrow {}^7F_{0,2,4}$). This indicates a substantial deviation from inversion symmetry (*21*). The presence of the strongly forbidden $^5D_0 \rightarrow {}^7F_0$ transition points to the presence of a relatively strong linear term in the crystal-field expression (*22*). The absence of inversion symmetry and the linear crystal-field term confirm the previous assignment of the C_{2v} site symmetry.

The extra line which shows up in the $^5D_0 \rightarrow {}^7F_2$ transition on the shorter wavelength side (see Figs. 3a, 3b, 3c, and 3d) is ascribed to another Eu^{3+} site of which the other lines are hidden under the main emission. From the spectra it follows that a small amount of this Eu^{3+} site is present in our samples. Excitation in the $^7F_0 \rightarrow {}^5L_6$ transition (Fig. 3e) reveals a Eu^{3+} site which does not show up under CT excitation. This site has either a very low efficiency under CT excitation, or its CT band is positioned at a wavelength that is too short to select with the xenon lamp. The fact that this possible CT band does not show up in the excitation spectrum recorded with the deuterium lamp points to a Eu^{3+} ion with very low efficiency under CT excitation, even at 4.2 K. The amount of Eu^{3+} ions that is incorporated in our samples on this particular site is comparable to the amount of Eu^{3+} ions on the C_{2v} site, since the magnetic dipole transition probabilities ($^5D_0 \rightarrow {}^7F_1$) are the same (*23*), and so are their intensities in the spectra (see Figs. 3e and 3f). Our results point, therefore, to the presence of at least three different types of Eu^{3+} ions in $CaSO_4:Eu^{3+}$.

The emission of Eu^{3+} in $CaSO_4:Eu^{3+}$, P^{5+} (Fig. 4) is very different from that of $CaSO_4:Eu^{3+}$. This suggests that the Eu^{3+} ions in the two phosphors are different. The $^5D_0 \rightarrow {}^7F_1$ magnetic dipole transition in the

case of $CaSO_4:Eu^{3+}$, P^{5+} has gained intensity, pointing to Eu^{3+} ions with site symmetry closer to inversion symmetry. A detailed study of the site symmetry is omitted here, but the presence of six lines in the $^5D_0 \rightarrow {}^7F_1$ transition points to at least two kinds of Eu^{3+} ions, since the maximum number of lines is only three. The fact that the CT bands are positioned at the same wavelength as in $CaSO_4:Eu^{3+}$ points to Eu^{3+} ions with similar oxygen surroundings. It is known that the amount of O atoms and the average Eu–O distance influence the position of the CT band (*24*).

The emission of Eu^{3+} in $CaSO_4:Eu^{3+},Na^+$ is again different from that of $CaSO_4:Eu^{3+}$ indicating a change of the surroundings of the Eu^{3+} ions in the crystal lattice. The seven lines that are observed in the $^5D_0 \rightarrow {}^7F_1$ transition with higher resolution (Fig. 4) must be due to at least three different Eu^{3+} sites in the lattice. The oxygen surroundings of the three sites are comparable, since their CT bands are positioned at the same wavelength (260 nm).

The characteristics of the spectra as they are discussed above show a strong effect of the charge compensators on the symmetry of the Eu^{3+} ions in the lattice. The strong influence of charge compensating effects on RE luminescence spectra has been studied by several authors (*25–30*). Model systems with high symmetric RE sites were investigated to facilitate the observation of the deviation from the RE site symmetries by charge compensators. The position of the charge compensators can be derived from the changing symmetry around the RE ions.

In our system is it hard to elucidate the exact symmetry of the RE sites. Hence it is impossible to deduce the exact location of the charge compensators. The character of the charge compensator, however, is indicative for its position in the crystal lattice. From the spectra of $CaSO_4:Eu^{3+},Na^+$ one dominating Eu^{3+} site is derived. This site is ascribed to Eu^{3+} ions that have a Na^+ ion nearby on the closest possible cation–cation distance in this lattice, viz. 3.5 Å. Then the Eu^{3+} ion and the Na^+ ion are linked through two O atoms. The two sites which are much weaker observable in $CaSO_4:Eu^{3+},Na^+$ most probably originate from Eu^{3+},Na^+ associates with larger distances (viz. 4.7 Å, where Eu^{3+} and Na^+ are linked through one O atom, and 5.8 Å, where Eu^{3+} and Na^+ are linked through a sulfate group). A similar assignment can be made for the two observed sites in $CaSO_4:Eu^{3+},P^{5+}$. The dominating Eu^{3+} site must be due to an Eu^{3+},P^{5+} associate with an interionic distance of 3.0 Å, where the two ions are linked together through two O atoms. The second site is ascribed to an Eu^{3+},P^{5+} associate at a distance of 3.6 Å, connected by one O atom.

In $CaSO_4:Eu^{3+}$ two dominating Eu^{3+} sites are observed (see Figs. 3e and 3f). One site has been ascribed already to an Eu^{3+} site with C_{2v} symmetry. This means that the Eu^{3+} ion replaces the Ca^{2+} ion without a distortion of the cation surroundings.The other site (observed only for excitation at 395 nm) is ascribed to an associate of an Eu^{3+} ion and a vacancy. The charge compensating mechanism on the cation sublattice includes the formation of one vacancy per two Eu^{3+} ions incorporated. The fact that the two dominating sites have a comparable concentration in the lattice shows that almost all vacancies are associated with Eu^{3+} ions.

In our laboratory the very inefficient composition $CaSO_4 \cdot 2H_2O:Eu^{3+}$ has also been studied (*31*). In this composition no influence of Na^+ on the luminescence spectra was observed. This was ascribed to the larger distance between the Ca^{2+} ions in this structure viz. 4.1 Å (*32*). This distance appears to be too large for a detectable influence of a compensator ion on the surrounding of the Eu^{3+} ion.

4.1.2 Quantum efficiency. The quantum efficiency of the Eu^{3+} luminescence of the phosphor $CaSO_4:Eu^{3+}$ was estimated with

a method described earlier (*31, 33*). This method is based on the fact that the transition probabilities of the $^7F_0 \rightarrow {}^5D_1$ magnetic dipole transition (*34*) and the CT transition (*35*) are not strongly influenced by the surroundings of the Eu^{3+} ion. We arrive at a total quantum efficiency for CT excitation of about 10% in the temperature region from 4.2 to 300 K which is independent of the Eu^{3+} doping concentration.

The quantum efficiency of the phosphor $CaSO_4:Eu^{3+}, P^{5+}$, determined by the same method, is about twice as high. The efficiency of the phosphor $CaSO_4:Eu^{3+}, Na^+$ is even higher, viz. 30%. Both efficiencies are independent of temperature. A confirmation of the different efficiencies found with this method is delivered by the excitation spectra at shorter wavelengths (Fig. 5). These spectra show the relative intensities of host lattice excitation toward CT excitation. If the host lattice excitation is considered to give a comparable quantum output of the Eu^{3+} luminescence for the three phosphors, the increase in CT excitation in the order $(Eu^{3+}) \rightarrow (Eu^{3+}, P^{5+}) \rightarrow (Eu^{3+}, Na^+)$ reflects an increase of the efficiency under CT excitation in the same direction.

From the emission spectra it was concluded that the Eu^{3+} ions are associated with the charge compensators. The different quantum efficiencies confirm this conclusion. Such associates have been reported before by Draai and Blasse (*16*) in $CaSO_4:Eu^{3+}, V^{5+}$ and Grasser *et al.* (*36*) in $CaWO_4:Sm^{3+}, Na^+$. The following explanation is proposed for the low values and the increase of the quantum efficiency. In the phosphor $CaSO_4:Eu^{3+}$ the extrinsic charge compensators are cation vacancies. If a vacancy, acting as a charge compensator, is positioned near a Eu^{3+} ion in the lattice, this Eu^{3+} ion can undergo a large relaxation in the excited CT state resulting into a low efficiency because of direct feeding of the ground state. Similar pronounced radiationless processes have been observed by Verwey *et al.* (*33*) for Eu^{3+} in glasses. The luminescence spectra of $CaSO_4:Eu^{3+}$ show one inefficient Eu^{3+} site which is most probably associated with a vacancy. If extrinsic charge compensators are present, the vacancy concentration will decrease and so will this inefficient site. This is exactly what we observe in the spectra of the phosphors $CaSO_4:Eu^{3+}, P^{5+}$ and $CaSO_4:Eu^{3+}, Na^+$. Only Eu^{3+} sites with comparable efficiencies show up, most probably originating from charge-compensated Eu^{3+} sites.

The quantum efficiencies of the charge-compensated phosphors are higher than that of the uncompensated phosphor, but are still relatively low in comparison with most Eu^{3+}-activated phosphors. This is ascribed to the fact that if trivalent cations are incorporated in a sublattice of divalent cations, they exert an extra attraction on the anions. In the CT state this extra attraction is no longer effective. This results in larger expansion, and thus a low quantum efficiency.

4.2 $CaSO_4:Ce^{3+}$

The very efficient luminescence of Ce^{3+} in $CaSO_4$ is in agreement with the very small Stokes shift of 800 cm^{-1}. As far as we know this is the smallest reported Stokes shift for the *d–f* transition of Ce^{3+}. The value of the Stokes shift is considered to be strongly dependent on the available space for the Ce^{3+} ion in the crystal lattice (*37*).

The smallest observed Stokes shift so far was reported for the Ce^{3+} ion in $ScBO_3$ (*37–39*) where the Ce^{3+} ion, with an ionic radius of 1.04 Å in VI coordination (*40*), replaces the Sc^{3+} ion (r_{VI} = 0.76 Å) in the calcite structure. It is remarkable that the Ce^{3+} ion in $CaSO_4$ (r_{VIII} = 1.14 Å), replacing the Ca^{2+} ion (r_{VIII} = 1.12 Å), has such a small Stokes shift, since the available space for the Ce^{3+} ion is much larger than in $ScBO_3$. This observation indicates that the radiationless relaxation in the excited state

is not solemnly governed by the available space for the Ce^{3+} ion.

A comparison of the Ce^{3+} luminescence efficiency with that of Eu^{3+} for excitation into the opposite-parity states shows the very different behavior of these excited states. Like the Eu^{3+} ion, the Ce^{3+} ion has an extra attraction for the surrounding anions. If the $4f$ electron of the Ce^{3+} ion is excited to a $5d$ orbital, the surrounding anions move even further toward the Ce^{3+} ion. This is due to the diffuse character of the $5d$ orbital (*41*). It is proposed that the further shrinking of the Ce^{3+} surroundings is restricted by repulsive forces between the coordinating anions. This means that the ground state and the excited state are only slightly different in equilibrium distance. Therefore, the Stokes shift and the radiationless relaxation rate for this d–f transition is small.

Returning to the luminescence spectra of the Ce^{3+} ion, we note a strong excitation band at 297 nm with a shoulder at 290 nm and three weaker ones at shorter wavelengths. According to the site symmetry of the Ce^{3+} ion, replacing the Ca^{2+} ion in $CaSO_4$, a fivefold splitting of the $5d$ level is expected. The crystal structure of $CaSO_4$ shows that the Ce^{2+} ion on a Ca^{2+} site has an oxygen coordination which can be considered as a distorted cube. In a cubic surrounding the threefold degenerate $5d$ level is split into a lower lying triplet T_{2g} and a doublet E_g (see Fig. 6). In C_{2v} site symmetry the degeneracies are lifted. Therefore, three bands are expected at the higher energy side, and two bands at the lower energy side. This is in agreement with the excitation spectrum of Fig. 6. It follows that the cubic crystal-field splitting amounts to about 5300 cm^{-1}. This value is of the same order as observed in several other systems (*38*).

The emission of Ce^{3+} in $CaSO_4$ consists of transitions from the lowest $5d$ level to the ^2F state which is split into $^2F_{5/2}$ (304 nm) and $^2F_{7/2}$ (325 nm). The splitting of the ^2F state amounts to 2100 cm^{-1} which is in agreement with the theoretical spin-orbit splitting. From group theoretical arguments it follows that the $^2F_{5/2}$ and the $^2F_{7/2}$ levels in C_{2v} site symmetry split into three and four crystal-field components, respectively. In the $5d \rightarrow {}^2F_{5/2}$ transition as well as in the $5d \rightarrow {}^2F_{7/2}$ transition two zero-phonon transitions are observed. In the $5d \rightarrow {}^2F_{5/2}$ emission band the two zero-phonon transitions have some phonon replicas at 237 (± 5) cm^{-1} from the electronic origin. It is likely that the third zero-phonon transition is hidden under the vibronic structure. Probably this accounts also for the absence of other zero-phonon transitions in the $5d \rightarrow {}^2F_{7/2}$ emission band.

In the excitation band which is ascribed to the transition from the $^2F_{5/2}$ state to the lowest energetic $5d$ level only one zero-phonon transition is observed. This is to be expected, since at 4.2 K only the lowest component of the $^2F_{5/2}$ state is occupied. The phonon replicas of the zero-phonon transition are at 218 (± 5) cm^{-1} from the electronic transition. The vibrational mode has a lower frequency in the excitation spectra than in the emission spectra indicating a weaker bonding in the excited state. The values of the observed vibrational frequencies in the progression mode point to a coupling of the electronic transition with the Ce–O bending vibration (*37*).

5. Conclusions

The Eu^{3+} luminescence in $CaSO_4$ under CT excitation is weak and the quantum efficiency amounts to about 10%. The quantum efficiency of the Eu^{3+} luminescence is enhanced in the presence of charge compensators. The P^{5+} ion, replacing the S^{6+} ion, increases the efficiency up to 20%.The Na^+ ion, positioned at a Ca^{2+} site, increases the efficiency even further (30%).

The improvement of the quantum efficiency can be explained from the replacement of vacancies by charge compensators.

Vacancies, situated near the Eu^{3+} ions, may give rise to a large offset of the excited CT state resulting in a high radiationless relaxation rate. Hence, the charge compensators, decreasing the amount of vacancies, increase the quantum efficiency under CT excitation. The charge compensators form associates with the Eu^{3+} ions in the lattice, indicating a local charge compensating effect.

In contrast to Eu^{3+} in $CaSO_4$, Ce^{3+} shows a very efficient luminescence, situated in the ultraviolet. The *d–f* luminescent transition of Ce^{3+} has a Stokes shift which amounts 800 cm^{-1}, the smallest value reported so far. In emission and excitation spectra vibrational structures are observed.

References

1. M. Buijs and G. Blasse, *J. Lumin.* **34,** 263 (1986).
2. G. Blasse and A. Bril, *J. Chem. Phys.* **45,** 3327 (1966).
3. G. Blasse, A. Bril, and W. C. Nieuwpoort, *J. Phys. Chem. Solids* **27,** 1587 (1966).
4. M. G. Zuev, *J. Lumin.* **21,** 217 (1980).
5. J. Huang, J. Loriers, and P. Porcher, *J. Solid State Chem.* **48,** 333 (1983).
6. T. Kano, K. Kinameri, and S. Sew, *J. Electrochem. Soc.* **129,** 2296 (1982).
7. G. Blasse and A. Bril, *Philips Res. Rep.* **21,** 368 (1966).
8. A. Bril, G. Blasse, and J. A. A. Bertens, *J. Electrochem. Soc.* **115,** 395 (1968).
9. F. A. Kröger, *in* "The Chemistry of Imperfect Crystals," 2nd ed., Vol. II, North-Holland/American Elsevier, Amsterdam (1974).
10. K. S. V. Nambi, *Phys. Status Solidi A* **83,** 175 (1984).
11. V. N. Bapat, *Phys. Status Solidi A* **54,** 171 (1979).
12. V. N. Bapat, *J. Phys. Chem.: Solid State Phys.* **10,** 465 (1977).
13. R. J. Danby, *J. Phys. Chem.: Solid State Phys.* **21,** 485 (1988).
14. K. S. V. Nambi and V. N. Bapat, *J. Phys. Chem.: Solid State Phys.* **13,** 1555 (1980).
15. R. J. Danby and N. B. Manson, *J.Chem. Phys.* **81,** 5462 (1984).
16. W. T. Draai and G. Blasse, *Phys. Status Solidi A* **21,** 569 (1974).
17. R. W. G. Wyckoff, *in* "Crystal Structures" Vol. III, p. 18, Interscience, New York (1965).
18. J. P.M. van Vliet and G. Blasse, *J. Electrochem. Soc.* **135,** 1574 (1988).
19. F. M. Ryan, W. Lehman, D. W. Feldman, and J. Murphy, *J. Electrochem. Soc.* **121,** 1475 (1974).
20. N. Yamashita, I. Yamamoto, K. Ninagawa, T. Wada, Y. Yamashita, and Y. Nakao, *Japan. J. Appl. Phys.* **24,** 1174 (1985).
21. G. Blasse, A. Bril, and W. C. Nieuwpoort, *J. Phys. Chem. Solids* **27,** 1587 (1966).
22. G. Blasse and A. Bril, *Philips Res. Rep.* **21,** 368 (1966).
23. G. Blasse, *Inorg. Chim. Acta,* **167,** 33 (1990).
24. H. E. Hoefdraad, *J. Solid State Chem.* **15,** 175 (1975).
25. M. P. Miller and J. C. Wright, *J.Chem. Phys.* **71,** 324 (1979).
26. B. M. Tissue and J. C. Wright, *Phys. Rev. B* **36,** 9781 (1987).
27. A. E. Hughes and G. P. Pells, *J. Phys. Chem.: Solid State Phys.* **7,** 3997 (1974).
28. R. J. Hamers, J. R. Wietfeldt, and J. C. Wright, *J. Chem. Phys.* **77,** 683 (1982).
29. S. K. Gayen and D. S. Hamilton, *Phys. Rev. B* **28,** 3706 (1983).
30. L. C. Porter and J. C. Wright, *J. Chem. Phys.* **77,** 2322 (1982).
31. D. van der Voort, G. Blasse, G. J. Witkamp, G. M. van Rosmalen, and L. H. Brixner, *Mater. Chem. Phys.*, **24,** 175 (1989).
32. M. Atoji and R. E. Rundle, *J. Chem. Phys.* **29,** 1306 (1958).
33. J. W. M. Verwey, G. J. Dirksen and G. Blasse, *J. Non-Cryst. Solids* **107,** 49 (1988).
34. W. T. Carnall, P. R. Fields, and K. Rajnak, *J. Chem. Phys.* **49,** 4412 (1968).
35. C. K. Jorgensen, *Mol. Phys.* **5,** 271 (1962).
36. R. Grasser, I. Jeuck, A. Scharmann, and J. Strode, *J. Lumin.* **40–41,** 389 (1988).
37. G. Blasse and G. J. Dirksen, *Inorg. Chim. Acta* **145,** 303 (1988).
38. G. Blasse and A. Bril, *J. Chem. Phys.* **47,** 5139 (1967).
39. T. Hoshina and S. Kuboniwa, *J. Phys. Soc. Japan.* **32,** 771 (1972).
40. R. D. Shannon, *Acta Crystallogr. A* **32,** 751 (1976).
41. G. Blasse, *J. Solid State Chem.* **9,** 147 (1974).